OPTIMAL LINEAR COMBINATION OF DENOISING SCHEMES FOR EFFICIENT REMOVAL OF IMAGE ARTIFACTS

Ramin Eslami and Hayder Radha

ECE Department / 2120 EB, Michigan State University, East Lansing, MI 48824, USA
Web: www.egr.msu.edu/waves

ABSTRACT

Different denoising schemes show dissimilar types of artifacts. For example, certain transform-based denoising schemes could introduce artifacts in smooth regions while others eliminate texture regions. Using different schemes for denoising a noisy image, we can consider the denoising results as different estimates of the image. Through linear combination of the results, we minimize the ℓ^2 norm of the error to find the optimum coefficients in a least-square-error sense. We employ the wavelet transform, contourlet transform, and adaptive 2-D Wiener filtering as our denoising schemes. Then we apply the proposed method to the denoising results of the individual schemes. This approach eliminates most of the artifacts and achieves significant improvement in the PSNR values. We also propose averaging of the denoising results as a special case of linear combination and show that it yields near-optimal performance.

1. INTRODUCTION

Wavelets have proven their capability in removing noise from a piece-wise smooth signal [12]. In wavelet denoising using hard thresholding, one simply set to zero the transform coefficients of a noisy signal that are below a threshold and reconstruct the resulting coefficients to obtain the denoised signal.

Recently, several new image transform schemes have been introduced, where most of them take advantage of the important feature of directionality [6]. Following a similar procedure to the wavelet denoising scheme, one can employ other transforms for denoising [9].

Owing to the characteristics of a transform, a transform-domain denoising scheme introduces some artifacts in the denoising results that are different from those of other schemes. Furthermore, each denoising scheme may have some advantages over the others and also some drawbacks. As a consequence, combination of different schemes would be a solution to reduce artifacts and compensate for the drawbacks. Taking advantage of the same idea, the authors in [5] proposed translation-invariant (TI) wavelet denoising, where it is, in fact, equivalent to the average of all denoised images resulting from the cycle-spinning algorithm. In [9] we have shown that the pseudo-Gibbs phenomena artifacts that usually appear in the denoising results when we use the contourlet transform denoising scheme, can be significantly reduced. In this paper, however, we use a different strategy that is based on a linear optimization approach in conjunction with employing *different* denoising schemes. Further, in this case, averaging is a special case of linear combination.

The remainder of the paper outline is as follows. In the next section we briefly highlight some of the related work. Section 3 provides problem formulation for our proposed linear combination method. In Section 4 we present the denoising schemes that we use in our experiments and examine their characteristics. The experimental results are provided in Section 5 and finally we provide our main conclusions in Section 6.

2. RELATED WORK

In a general framework, when one wishes to find an optimal representation over a *dictionary* of bases functions, a few algorithms have been proposed [10]. Suppose that $\mathcal{D}=[\mathcal{B}_1,...\mathcal{B}_K]$ is the dictionary of the bases functions, where $\mathcal{B}_i$ is the matrix corresponding to the ith basis and we want to decompose a signal x (given in a column vector of length N) using the dictionary $\mathcal{D}$. Therefore, we have

$$x=\mathcal{B}\alpha \quad (\alpha=[\alpha_1,...,\alpha_N]^T),$$

where α is the array of the coefficients and $(\cdot)^T$ denotes the transpose operation. The *method of frames* [12], provides an α with a minimized ℓ^2 norm. *Basis pursuit* [4] is another algorithm, which optimizes α subject to ℓ^1 norm; and hence, results in a linear programming approach. *Matching pursuit* [13] attempts to find a *best* basis in $\mathcal{D}$ utilizing a greedy algorithm. It sequentially adds elements from $\mathcal{D}$ that are most correlated with the residual. The above methods, however, are computationally expensive.

Total variation is a technique employed to denoising [15] and later was combined to the wavelet scheme to reduce artifacts in wavelet denoising [3][8]. Using the same idea, the authors in [2] applied the curvelet transform in conjunction with total variation to improve the denoising results of curvelets. Starck *et al*. [16] proposed an algorithm to combine several transforms, where they used an iterative approach to minimize an ℓ^1 norm instead of total variation norm.

Our approach, however, is based on a linear combination of the denoising results and thus is not complex. Meanwhile, the proposed approach provides improvement in the PSNR

values and, more importantly, in visual quality due to significant reduction of the artifacts.

3. PROBLEM FORMULATION

We wish to find an analytical solution to the following problem. Suppose that **V** is a normed linear vector space and $S=\{x_0,x_1,...,x_{K-1}\}$ is a set of linearly independent vectors in space **V**. Given a vector $s\in\mathbf{V}$, we would like to find the coefficients $\{c_i\}_{0\le i<K}$ in such a way to minimize the error $\|e\|=\|s-\hat{s}\|$, where $\hat{s}=\sum_{i=0}^{K-1}c_i x_i$ is the estimation of *s*. If we use the ℓ^2 norm, it leads to minimizing the MSE (mean-squared error). We achieve the minimum error if it is orthogonal to span(*S*), i.e., it is orthogonal to the data used to estimate the signal *s*:

$$\langle e,x_j\rangle=\left\langle s-\sum_{i=0}^{K-1}c_i x_i,\ x_j\right\rangle=0,\ \text{for } j=0,1,...,K-1,$$

where $<,>$ denotes the inner product.

This leads to $\mathbf{Rc}=\mathbf{P}$, where **R** is the Grammian matrix and **P** is the cross-correlation matrix as defined below [14]:

$$\mathbf{R}=\begin{bmatrix}\langle x_0,x_0\rangle & \langle x_1,x_0\rangle & \cdots & \langle x_{K-1},x_0\rangle\\ \langle x_0,x_1\rangle & \langle x_1,x_1\rangle & \cdots & \langle x_{K-1},x_1\rangle\\ \vdots & & & \vdots\\ \langle x_0,x_{K-1}\rangle & \langle x_1,x_{K-1}\rangle & \cdots & \langle x_{K-1},x_{K-1}\rangle\end{bmatrix},$$

$$\mathbf{P}=\begin{bmatrix}\langle s,x_0\rangle & \langle s,x_1\rangle & \cdots & \langle s,x_{K-1}\rangle\end{bmatrix}^T,$$

and $\mathbf{c}=[c_0\quad c_1\quad\cdots\quad c_{K-1}]^T$.

If the vectors in the set *S* are linearly independent, the Grammian matrix **R** is positive-definite and hence, is invertible. Therefore, we have the solution $\mathbf{c}=\mathbf{R}^{-1}\mathbf{P}$ for the unknown coefficients in **c**.

For our problem, we consider *s* as the original image, and $z=s+\nu$ as the image corrupted with additive Gaussian noise ν. Then we apply *K* different image denoising schemes to obtain $S=\{x_0,x_1,...,x_{K-1}\}$ as the set of different denoised images and obtain $\hat{s}$ as the denoised image using the above least mean-squared (LMS) approach.

Note that here, to find the coefficient vector **c**, we need to have the original signal *s* to compute **P**. That is, the above optimal approach is an *oracle* method, which gives the *lower bound* of the estimation error. Meanwhile, since *z* is the maximum likelihood estimation of *s* [1], we can use this noisy image instead of the original. In that case, the elements of **P** will be

$$\begin{aligned}\langle z,x_i\rangle&=\langle s+\nu,x_i\rangle\quad(0\le i<K)\\&=\langle s,x_i\rangle+\langle \nu,x_i\rangle.\end{aligned}$$

If we define the inner product for random variables as expectation, we have $\langle \nu,x_i\rangle=E[\nu x_i]$, which is not zero because the remaining noise in the estimates $\{x_i\}_{0\le i<K}$ is colored and correlated with ν. However, when the power of input noise is low, this term is close to zero.

The other way to omit the role of *s* in **P** is to weight all denoised images, equally: $\hat{s}_{ave}=(1/K)\sum_{i=0}^{K-1}x_i$. Indeed, if the remained noise in $\{x_i\}_{0\le i<K}$, i.e. $\tilde{v}_i=x_i-s$, $(0\le i<K)$, were white and they were independent from each other, the maximum likelihood estimation of *s* given $\{x_i\}_{0\le i<K}$ would become $\hat{s}_{ave}$ [11 p. 569]. Nevertheless, although $\{\tilde{v}_i\}_{0\le i<K}$ do not satisfy the above conditions, our results show that averaging is an efficient approach when the denoised images are of comparable quality.

4. CHARACTERISTICS OF SOME IMAGE DENOISING SCHEMES

In our experiments, we use three different denoising techniques[1]: the wavelet denoising [12], the contourlet denoising [9], and the adaptive Wiener filtering [11 p. 536]. In the case of wavelets and contourlets, we also consider their translation-invariant schemes [5][9]. Below, we briefly describe the characteristics of these schemes for image denoising.

4.1 Wavelet Denoising Scheme

The wavelet transform has shown its capability for denoising piece-wise smooth images [12]. Wavelets, indeed, provide unconditional bases of ℓ^2 and also of many smoothness spaces [7]. As a result, wavelet shrinkage is a smoothing operation for a wide variety of signal classes. Wavelet shrinkage in comparison to other older methods such as convolutional smoothers and Fourier-domain damping is much simpler, and offers many broad near-optimality properties not achievable by the older methods [7].

An important problem that arises in a transform-domain denoising is the artifacts introduced when one thresholds the transform coefficients. The artifacts are in fact due to pseudo-Gibbs phenomena, which occur near edges and discontinuities and resemble the basis functions of the transform. Fig. 1(a) shows some of the basis functions of the wavelet transform. Since this transform is efficient in capturing point-wise singularities, the basis functions are like points. Therefore, the artifacts in a denoised image will look like the basis functions as shown in Fig. 1(b), which depicts an example, where the standard deviation of input noise is 20. Notably, this denoising scheme is incapable of capturing some textures and fine details.

4.2 Contourlet Denoising Scheme

The contourlet transform, one of the geometrical image transform, is introduced to better capture directional features of an image [6]. It is constructed using two filter bank stages: Laplacian pyramids and directional filter banks. The Laplacian pyramid is a multiresolution scheme, which acquires the feature of directionality in the contourlet transform using the directional filter banks. Owing to the directionality of this transform, the basis functions are in the form of needle-shaped segments, which can be oriented in different directions as

[1] Note that the proposed approach is applicable to any set of denoising schemes.

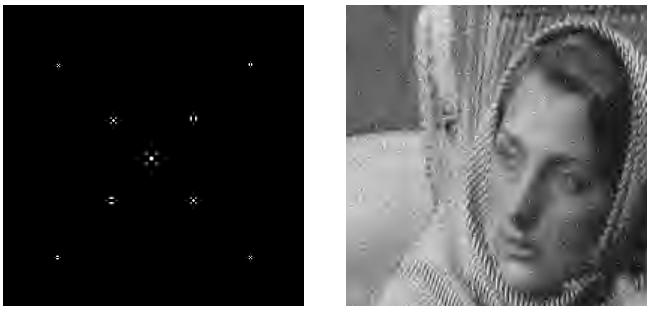

(a) (b)

Fig. 1. (a) Some basis functions of wavelets. (b) The denoising result of the *Barbara* image using wavelets where $\sigma_v = 20$.

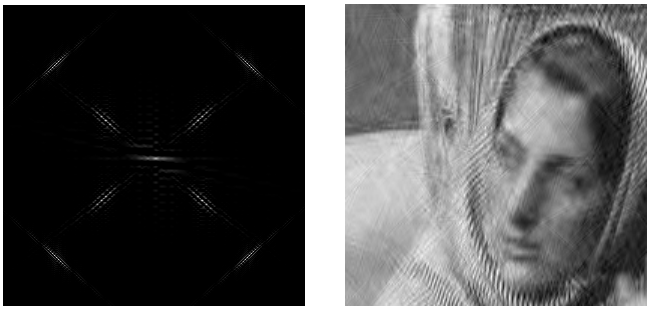

(a) (b)

Fig. 2. (a) Some basis functions of contourlets. (b) The denoising result of the *Barbara* image using contourlets where $\sigma_v = 20$.

Fig. 2(a) shows. Consequently, the denoising artifacts will look like arbitrarily-oriented needle-shaped segments that are more visible in the smooth regions (see Fig. 2(b)). To have sufficient directional resolution, one has to use directional filters with large support. As a result, the basis functions and thus the artifacts appear in the form of long segments, which severely degrade the quality of the denoised image. Nevertheless, the contourlet denoising scheme outperforms the wavelet approach in retaining textures and fine details in the denoising results (compare Figs. 1(b) and 2(b)).

4.3 Adaptive Wiener Filtering

The Wiener filtering is a traditional denoising method, which usually leads to a lowpass filtration. This approach would be the optimal linear minimum mean square error estimate of the signal if $s[n]$ and $v[n]$ ($n = (n_1, n_2)$) are samples of stationary random processes that are linearly independent from each other and their *power spectral densities* (PSD) are known [11]. Practically, however, the above assumptions do not hold. To improve the performance of this scheme, we can use adaptive filtering, where one locally estimates the PSDs of the signal and noise and estimates the signal. As a result, if $m_z^{(\Omega)}$ and $\sigma_z^{2(\Omega)}$ denote the local minimum and variance of the noisy image z in the window Ω, respectively, the local estimate $\hat{s}^{(\Omega)}$ is [11]

$$\hat{s}^{(\Omega)} = m_z^{(\Omega)} + \frac{\sigma_z^{2(\Omega)} - \sigma_v^2}{\sigma_z^{2(\Omega)}} \left(z^{(\Omega)} - m_z^{(\Omega)} \right),$$

where we assumed that v is a zero-mean white Gaussian noise.

TABLE I
PSNR VALUES OF THE DENOISED IMAGES WHEN $\sigma_v = 20$

Method	Noisy	WT	CT	AWF	LMS_O	LMS_N	AVE
Barbara	22.15	25.70	26.31	26.43	27.86	27.69	27.81
Boats	22.18	27.14	26.83	28.38	29.20	28.91	29.06
GoldHill	22.18	26.87	26.66	28.65	29.03	28.81	28.72
Mandrill	22.13	22.98	22.66	23.55	24.41	24.38	24.38
Peppers	22.32	28.41	27.69	30.12	30.67	30.22	30.30

WT: Wavelet Transform, LMS_O: LMS with oracle,
CT: Contourlet Transform, LMS_N: LMS using noisy image,
AWF: Adaptive Wiener Filter, AVE: Averaging

Since this approach is a locally filtering task, it introduces artifacts, which resemble speckle noise (Fig. 3(a)). As we enlarge the window size, the artifacts reduce, but more edges are smeared in the denoised image.

Compared with the wavelet and contourlet denoising schemes, this approach provides competitive results. In comparison with the translation-invariant (TI) wavelet and contourlet schemes [9], however, this scheme yields poor performance. Consequently, we merely take advantage of the wavelet and contourlet schemes for linear combination when we use TI denoising.

5. EXPERIMENTAL RESULTS

To test our proposed LMS approach, we selected a variety of images and used additive Gaussian noise with $\sigma_v = 20$ and 40. We employed the same wavelet and contourlet schemes as in [9] and applied hard thresholding with a threshold equal to $3\sigma_v$. For adaptive Wiener filtering, we used a window size of (5,5). We also utilized our approach for TI denoising. Note that we obtain better results in this case at the expense of more computational complexity.

Table I provides the PSNR values when $\sigma_v = 20$. As seen, the proposed LMS method achieves more than one dB improvement in some cases. The results where the noisy image is used as the estimate of the original signal in the LMS algorithm (LMS_N) are comparable with the LMS_O (LMS with oracle) results. Interestingly, the averaging approach (AVE) provides near-optimal PSNR values (recall that the LMS_O provides optimal results). Note that although the PSNR values achieved using adaptive Wiener method are usually higher than those of the wavelet and contourlet schemes, it introduces more visible artifacts in the results. That is due to the fact that the PSNR measure treats the low-frequency artifacts similar to the high-frequency ones; while, eyes are usually more sensitive to the low-frequency artifacts.

Table II shows the PSNR results when $\sigma_v = 40$. Since the noise power is higher in this case, the noisy image is a poor estimate of the original image and hence, the LMS_N approach results in poor performance. Remarkably, the averaging method yields near-optimal performance again.

Fig. 3 depicts the visual results of the *Barbara* image where we already observed the denoising results using wavelets and contourlets schemes in Figs. 1 and 2. In this figure ((b), (c), and (d)), we see that the artifacts introduced by the individual denoising schemes are significantly reduced while the salient

TABLE II
PSNR VALUES OF THE DENOISED IMAGES WHEN $\sigma_v = 40$

Method	Noisy	WT	CT	AWF	LMS_O	LMS_N	AVE
Barbara	16.39	22.48	23.04	23.65	24.61	22.94	24.49
Boats	16.43	23.93	23.67	25.13	26.03	23.66	25.86
GoldHill	16.42	23.98	23.85	25.55	26.28	23.68	25.98
Mandrill	16.37	20.21	20.14	21.81	22.03	21.57	21.73
Peppers	16.60	24.70	24.26	25.81	26.77	23.59	26.56

advantages of these schemes are preserved. Further, the LMS_N and AVE (averaging) methods provide competitive results to those of the optimal LMS_O approach. Another example is demonstrated in Fig. 4, where we used TI wavelet (TIWT) and contourlet (TICT) denoising schemes [9] with $\sigma_v = 40$. As shown, the averaging performance is almost the same as the LMS_O method. The result of the proposed approach shows fewer artifacts and better PSNR values.

6. CONCLUSION

In this paper we proposed a method based on the least mean-squared approach to linearly combine different denoising schemes in an optimal sense. We found the proposed scheme to be efficient in improving denoising results through significant reduction in the artifacts and hence an increase in the PSNR values. We also proposed averaging as a special case of linear combining, where we achieved near-optimal results while maintaining low complexity.

7. REFERENCES

[1] P. J. Bickel K. A. Doksum, *Mathematical Statistics: Basic Ideas and Selected Topics.* Oakland, CA, Holden-Day, 1977.

[2] E. Candès and F. Guo, "New Multiscale Transforms, Minimum Total Variation Synthesis: Applications to Edge-Preserving Image Reconstruction," *Signal Processing.* **82**, pp. 1519-1543.

[3] T. F. Chan and H. M. Zhou, "Optimal Construction of Wavelet Coefficients Using Total Variation Regularization in Image Compression," *CAM Technical report*, UCLA, 2000.

[4] S. Chen and D. Donoho, "Atomic Decomposition by Basis Pursuit," *in SPIE Int'l. Conf. on Wavelets*, Jul. 1995.

[5] R. R. Coifman and D. L. Donoho, "Translation Invariant De-noising," *in Wavelets and Statistics, Springer Lecture Notes in Statistics 103*, New York, Springer-Verlag, pp. 125-150, 1994.

[6] M. N. Do, *Directional Multiresolution Image Representations.* Ph.D. thesis, EPFL, Lausanne, Switzerland, Dec. 2001.

[7] D. L. Donoho, "Nonlinear Wavelet Methods for Recovery of Signals, Densities, and Spectra from Indirect and Noisy Data" in *proc. of Symposia in Applied Math.,* pp. 173-205, 1993.

[8] S. Durand and J. Froment, "Artifact Free Signal Denoising with Wavelets," *in proc. of IEEE ICASSP*, pp. 3685-3688, 2001.

[9] R. Eslami and H. Radha, "Image Denoising Using Translation-Invariant Contourlet Transform," *in proc. of IEEE ICASSP*, vol. 4, pp. 557-560, Philadelphia, PA, Mar. 2005. Available online at www.egr.msu.edu/~eslamira .

[10] X. Huo, *Sparse Image Representation via Combined Transforms.* Ph.D. thesis, Stanford University, Aug. 1999.

[11] J. S. Lim, *Two-Dimensional Signal and Image Processing.* Prentice Hall, 1990.

[12] S. Mallat, *A Wavelet Tour of Signal Processing.* Academic Press, 2nd Ed., 1998.

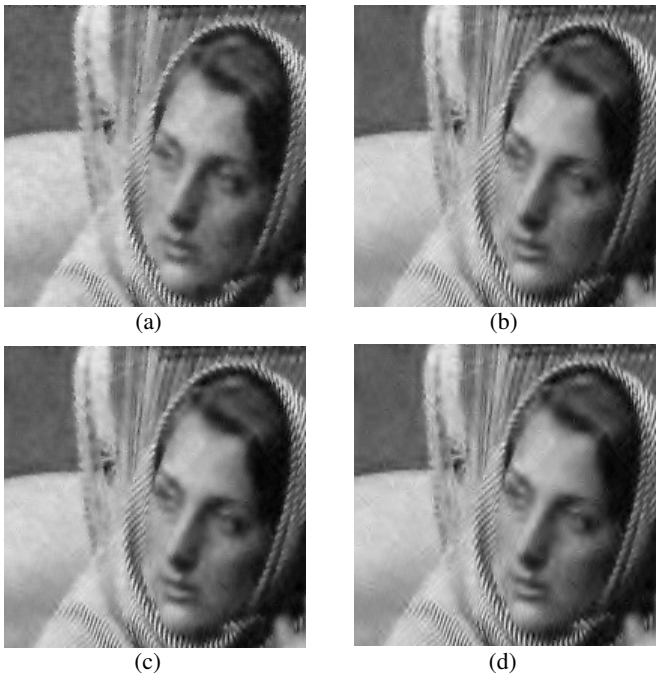

(a) (b) (c) (d)

Fig. 3. The denoising results of the *Barbara* image when $\sigma_v = 20$ using methods: (a) AWF. (b) LMS_O. (c) LMS_N. (d) AVE. (see also Figs. 1(b) and 2(b) for the results of other schemes).

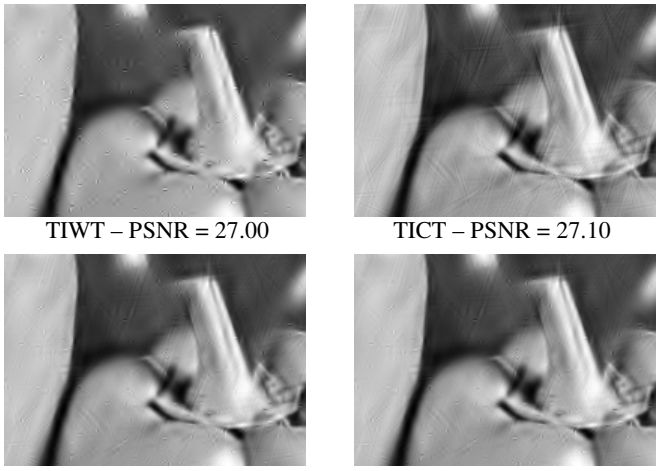

TIWT – PSNR = 27.00 TICT – PSNR = 27.10

LMS_O – PSNR = 27.344 AVE – PSNR = 27.341

Fig. 4. The denoising results of the *Peppers* image when $\sigma_v = 40$ using translation-invariant schemes.

[13] S. Mallat and Z. Zhang, "Matching Pursuit with Time-Frequency Dictionaries," *IEEE Trans. Signal Processing*, vol. 41, pp.3397-3415, Dec. 1993.

[14] T. K. Moon and W. C. Stirling, *Mathematical Methods and Algorithms for Signal Processing.* Prentice Hall, 2000.

[15] L. I. Rudin, S. Osher, and E. Fatemi, "Nonlinear Total Variation Based Noise Removal Algorithm," *Physica D*, 60, pp. 259–268, 1992.

[16] J. L. Starck, D. L. Donoho, and E. Candes, "Very High Quality Image Restoration," *in SPIE Conf. on Signal and Image Proc.: Wavelet Apps. in Sig. and Image Proc. IX,* vol. 4478, 2001.